Chemistry - A European Journal 23.18 (2017): 4320-4326

DOI: https://doi.org/10.1002/chem.201605285

Photoantimicrobial Biohybrids by Supramolecular Immobilization of Cationic Phthalocyanines onto Cellulose Nanocrystals

Eduardo Anaya-Plaza,[a] Eveline van de Winckel,[a] Joona Mikkilä,[b] Jani-Markus Malho,[c] Olli Ikkala,[c] Oscar Gulías,[d] Roger Bresolí-Obach,[d] Montserrat Agut,[d] Santi Nonell,[d] Tomás Torres,*[a] Mauri A. Kostiainen,*[b] Andrés de la Escosura*[a]

Abstract: The development of photoactive and biocompatible nanostructures is a highly desirable goal to address the current threat of antibiotic resistance. Herein, we describe a novel supramolecular biohybrid nanostructure based on the non-covalent immobilization of cationic zinc phthalocyanine (ZnPc) derivatives onto unmodified cellulose nanocrystals (CNC), following an easy and straightforward protocol where binding is driven by electrostatic interactions. These non-covalent biohybrids show strong photodynamic activity against *S. aureus* and *E. coli*, representative examples of Gram-positive and Gram-negative bacteria, respectively, and *C. albicans*, a representative opportunistic fungal pathogen, outperforming the free ZnPc counterparts and related nanosystems in which the photosensitiser is covalently linked to the CNC surface.

Introduction

Molecular and nanostructured materials based on organic dyes such as porphyrins and phthalocyanines (Pc) are widely used in materials science and nanotechnology.[1–4] Key properties of Pc include high stability and absorption coefficients at the near-infrared (NIR) spectral window, long-lived fluorescence, a rich electrochemistry, and high quantum yields of photoinduced singlet oxygen ($^1O_2$) generation (Φ_Δ).[5–11] Such properties are also key features of photoantimicrobials, i.e., antimicrobial drugs that are activated by light.[12] Photoantimicrobials are an emerging type of drugs that are currently being actively investigated to address the growing threat of antibiotic resistance.[13–15] Yet, Pc tend to self-aggregate, especially in aqueous conditions, where *H*-type stacks are normally formed.[16] This kind of aggregation leads to self-quenching of the excited state, limiting the applicability of these macrocycles. A growing strategy to circumvent such limitation consists in using biological nanostructures to create bioinspired hybrid materials where the optical properties of the chromophore are maintained or even enhanced. The field of Pc-based biohybrid materials is at a very early stage of research, but a number of biological nanostructures have been utilized toward this end, including peptides, antibodies, protein cages, DNA, liposomes and carbohydrates.[5,9–11,16–24] Herein, we describe the immobilization of cationic zinc Pc (ZnPc) derivatives on the sulphated surface of pristine cellulose nanocrystals (CNC) through an easy, non-covalent approach (Figure 1), resulting in well-defined nanostructured Pc systems. Importantly, and because of the employed supramolecular strategy, the Pc photodynamic properties, normally hindered in aqueous media due to aggregation, are preserved in the resulting complexes, as demonstrated by their capacity to efficiently kill Gram-positive and Gram-negative bacteria and a pathological yeast.

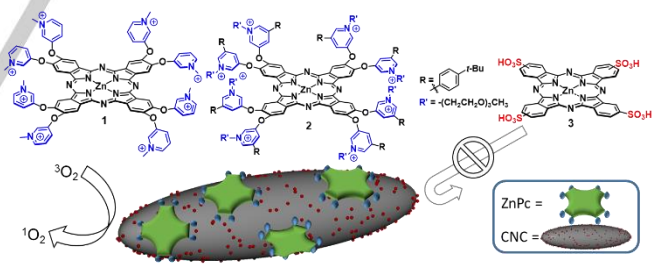

Figure 1. Chemical structure of the cationic ZnPc derivatives **1** and **2**, and the anionic ZnPc **3**, used as negative control (*top*). Schematic representation of ZnPc immobilized supramolecularly onto the surface of sulphate-decorated CNC, as an example of nanostructured, biohybrid singlet oxygen generators (*bottom*).

Cellulose, being the most abundant biopolymer produced in the biosphere, has been industrially processed and used for nearly 150 years. However, in the last two decades, nanoscience has enabled the development of new high-end cellulose derivatives from renewable resources. Rod-shaped CNC have attracted growing attention due to their extraordinary mechanical properties, high aspect ratio and surface area, colloidal stability, biocompatible sugar-based chemical structure and cheap processing for a well-defined

[a] Dr. E. Anaya-Plaza, E. van de Winckel, Prof. T. Torres and Dr. A. de la Escosura
Departamento de Química Orgánica (C-I)
Universidad Autónoma de Madrid / IMDEA (TT)
Cantoblanco 28049, Madrid (Spain)
Fax: (+34) 91-497-3966
E-mail: tomas.torres@uam.es; andres.delaescosura@uam.es
Homepage: http://www.uam.es/gruposinv/ftalo
[b] J. Mikkila and Prof. M. A. Kostiainen
Department of Biotechnology and Chemical Technology
Aalto University
00076, Aalto, Finland
[c] Dr. J. -M. Malho and Prof. O. Ikkala
Department of Applied Physics
Aalto University
00076, Aalto, Finland
[d] O. Gulías, R. Bresolí-Obach, Prof. M. Agut and Prof. S. Nonell
Institut Químic de Sarrià
Universitat Ramon Llull
08017 Barcelona (Spain)

Supporting information for this article is given via a link at the end of the document.

nanomaterial.[25–30] Different CNC functionalization procedures have been described,[31] commonly starting with a covalent modification of the CNC surface, in order to provide reactive functional groups or supramolecular recognition motifs.[32–36] Among them, only few examples have exploited CNC in combination with dyes, mainly porphyrinoids and ruthenium complexes, for catalytic or biomedical applications.[24,36–42]

Our strategy to decorate CNC with Pc molecules relies on the octacationic zinc Pc (ZnPc) derivatives **1** and **2**, which can bind through electrostatic interactions to the negatively charged surface of sulphated CNC. The selected ZnPc compounds present eight pyridinium moieties that, in the case of **2**, are quaternized with a methoxy(triethylenoxy) chain to further enhance hydrophilicity. Compound **2** also presents *tert*-butylphenyl substituents at the 5-position of the pyridinium units, as bulky aliphatic rests that tune aggregation in aqueous solution. The anionic ZnPc **3** was employed as negative control, showing no functionalization of the CNC. The present studies thus demonstrate that anion-cation recognition is a suitable driving force to produce ZnPc-CNC hybrids in an easy and straightforward manner. Moreover, the photochemical properties of these supramolecular complexes suggest their potential toward biomedicine and nanotechnology applications.

Results and Discussion

CNC with negatively charged surface sulphate groups were isolated from filter paper by sulfuric acid hydrolysis (see SI).[43] The ZnPc compounds **1**[44] and **3**[45] were prepared as reported previously, and showed high solubility in water. The synthesis of **2** is described in the experimental section and Figure S1. Owing to the *tert*-butylphenyl groups, compound **2** presents a poorer solubility in aqueous media compared to **1**. The ZnPc-CNC hybrids, in turn, were easily prepared by ultrasound bath-assisted dispersion of the CNC (5 mg mL^{-1}, 3 mL) in the corresponding ZnPc aqueous solution (ca. 0.1 mM, 12 mL) for 30 min. The samples were then centrifuged at 10000 rpm (9391 rfc) for 10 min and the pellets were washed five times with water and centrifuged again, until no colour was observed in the supernatant. Importantly, for the reference compound **3**, the resulting sample did not show any ZnPc UV-Vis absorption bands after redispersion in water or phosphate buffer saline (PBS), demonstrating that in this case there was no CNC functionalization and the pristine CNC were recovered. As a consequence, the next paragraphs will focus on the full characterization of hybrids **1-CNC** and **2-CNC**.

The ZnPc payload in the hybrids was determined through elemental analysis of lyophilized **1-CNC** (C, 43.0; H, 6.2; N, 0.23%) and **2-CNC** (C, 43.6; H, 6.14; N, 0.36%). By comparison with the molecular formulae of pristine CNC $(C_6H_{10}O_5)_n$, **1** ($C_{80}H_{64}O_{24}N_{16}S_4Zn$) and **2** ($C_{208}H_{256}O_{32}N_{16}I_8Zn$), combined in different ratios, the ZnPc payload in **1-CNC** and **2-CNC** was calculated to be 1.0 x 10^{-5} and 1.7 x 10^{-5} mol of ZnPc per gram of CNC, respectively (see SI). The binding efficiency was then evaluated for **1-CNC** (13.5%) and **2-CNC** (22.2% of sulphate groups neutralized by the ZnPc cationic charges) by comparing the ZnPc payload and the sulphate ester degree of substitution, previously determined as 0.1 (Table S1).[35]

Next, we proceeded to study the aggregation behaviour of **1** and **2**, both in solution and bound onto the CNC, by UV-Vis spectroscopy in different solvents (Figure 2). In MeOH, both compounds exist in their monomeric form, displaying a characteristic sharp and intense absorption band at 670 nm and 674 nm, respectively, as is also the case for **1** in water. In turn, **2** shows the appearance of a strong absorption band at 635 nm in water, an indication of *H*-type ZnPc aggregation.[46]. In aqueous PBS, a physiologically relevant medium, the intensity of this band increases at the expense of the monomer band. Interestingly, **1** appears to be more aggregated than **2** (Figure 2). The absorption spectra of the ZnPc-CNC hybrids **1-CNC** and **2-CNC** in methanol and water, on the other hand, show the characteristics of non-aggregated ZnPc (i.e., lack of the absorption band at 635 nm), as well as the typical scattering from CNC over the whole spectral range. In PBS all CNCs showed aggregation of the ZnPc, though to a lower extent than **1** and **2**. These results are consistent with **2** being more hydrophobic than **1**, hence more prone to aggregation in aqueous media, but also with higher steric hindrance, which leads to a weaker intermolecular electronic coupling in the aggregates. It is worth noting that the ZnPc molecules remain anchored to the CNC surface even in MeOH, as the solutions obtained by centrifugation are colourless (Figure S2).

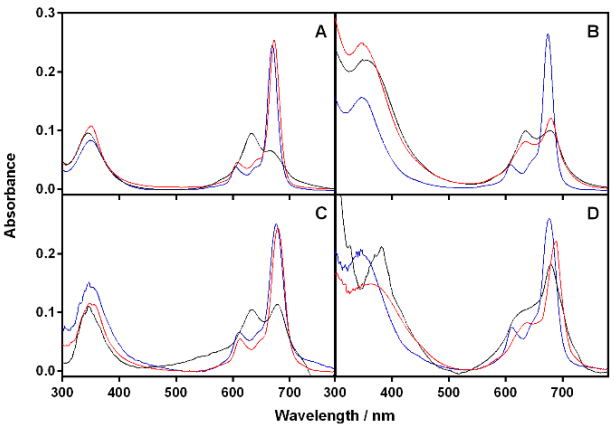

Figure 2. Absorption spectra of compounds 1 (A), 2 (B) in methanol (blue), water (red) and PBS (black), as compared to those of hybrids 1-CNC (C) and 2-CNC (D).

The robustness of the present non-covalent ZnPc-CNC hybrids was also evaluated by thermogravimetric analysis (Figure S3). Pristine CNC start to decompose above 200 °C,

owing to a catalytic effect that was previously assigned to the surface sulphate groups.[47] On the other hand, decomposition of **1-CNC** and **2-CNC** only starts above 300 °C, suggesting that the catalytic effect is hindered in the hybrids, and further highlighting the interaction between sulphate moieties and cationic ZnPc as the binding driving force.

Dynamic light scattering (DLS) was used to estimate the hydrodynamic diameter of pristine CNC (128 ± 8 nm), **1-CNC** (234 ± 17 nm) and **2-CNC** (216 ± 17 nm), at low concentration (0.05 mg mL^{-1}) to minimize the absorption of the ZnPc (Figure 3a). A significant increase in size can be observed for the complexes in comparison to pristine CNC (Table 1). We ascribe this size increase to a slight CNC aggregation and electrostatic cross-linking induced by the immobilized ZnPc, consistent with the solvent effect on the absorption spectra. Yet the particle sizes remain in the range of a few hundreds of nanometres and have moderate polydispersity index (PDI) values.

Table 1. Z-average size and PDI from DLS, mobility and ζ-potential measurements of CNC, **1-CNC** and **2-CNC**.

	Z-avg. / nm	PDI	Mobility / 10^{-8} $m^2 \cdot V^{-1} \cdot s^{-1}$	ζ-Pot. / mV
CNC	128±8	0.18	-3.23±0.04	-41.3±5.5
1-CNC	234±17	0.34	-3.20±0.2	-40.4±2.3
2-CNC	216±17	0.24	-0.93±0.12	-12.0±1.5

The electric double layer of the system was evaluated by measuring the electrophoretic mobility (Table 1) and ζ-potentials (Figure 3b) of the hybrid particles at 0.05 mg mL^{-1}. The value found for **1-CNC** (-3.20 x 10^{-8} m^2 V^{-1} s^{-1}) closely resembles that of the pristine CNC (-3.23 x 10^{-8} m^2 V^{-1} s^{-1}), as a consequence of the low percentage of interacting sulphate esters (13.5%) in **1-CNC**, which leaves the electrostatic surface of the particles very similar to that in the absence of ZnPc. On the contrary, the electrophoretic mobility of **2-CNC** (-0.93 x 10^{-8} m^2 V^{-1} s^{-1}) drops drastically, as compared to pristine CNC. We ascribe this effect to the methoxy(triethylenoxy) chains, which render a more neutral solvation sphere and colloidal stabilization of the particle surface.

In order to characterize the aggregation of the ZnPc-decorated CNC, suggested above by DLS data, electron microscopy studies were also conducted. Cryogenic transmission electron microscopy (cryo-TEM) images of **1-CNC** (Figure 3c) show clusters of slightly aggregated rod-shaped nanocrystals in different orientations. This behaviour differs from **2-CNC** (Figure 3d) where all the nanocrystals are shown in flat, highly orientated, well-packed sheets. We ascribe these differences to the presence of PEG chains in the chemical structure of **2** that hinder the binding kinetics to the CNC, favouring the formation of closed-packed assemblies. In opposition, the exposed cationic surface of **1** binds fast and crosslinks CNCs into amorphous aggregates.

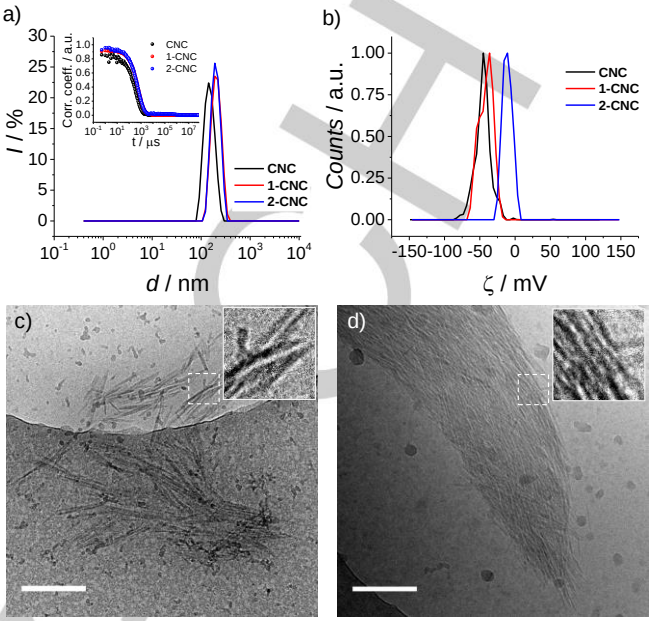

Figure 3. (a) DLS results showing the increase in intensity-averaged size distribution when CNC are coated with **1** (**1-CNC**) and **2** (**2-CNC**) in 5 µg/L solutions. *Inset*: correlograms of selected spectra. (b) ζ-potential of CNC showing no variation in **1-CNC** and a decrease of 29.3 mV in absolute value for **2-CNC**. Cryo-TEM image of (c) **1-CNC** and (d) **2-CNC** at 0.5 mg/mL in water. Scale bars: 200 nm. Insets show magnifications of the areas marked by dashed lines.

To demonstrate the photoactive character of the ZnPc-CNC complexes, we proceeded to study their efficacy for photoinduced $^1O_2$ production and to compare it with that of the corresponding free ZnPc references. To this end, time-resolved near-IR spectroscopy was used to monitor the phosphorescence of $^1O_2$ at 1275 nm and compare it to that of suitable references (see Table 2 and Figure S4).[48] The results show that **1** is an intrinsically better photosensitiser than **2** in methanol, where both are in monomeric form. In PBS both compounds lose their photosensitising ability due to extensive aggregation. An intermediate behaviour is observed in neat D_2O, used instead of H_2O to increase the $^1O_2$ lifetime,[49] namely **1** behaves as in methanol but **2** is closer to PBS due to its more hydrophobic character.

Table 2. $^1O_2$ quantum yield (Φ_Δ) values determined in various solvents. All Φ_Δ values were determined as the average of three different measurements.

	Φ_Δ [MeOH]	Φ_Δ[H_2O]	Φ_Δ [PBS]
1	0.62±0.03	0.74±0.06	0.04±0.01
1-CNC	0.02±0.01	~0.01	<0.01
2	0.20±0.04	0.04±0.01	<0.01
2-CNC	0.02±0.01	~0.01	<0.01

Contrary to what could perhaps be expected in view of the almost pure monomeric absorption spectra (cf. Figure 2), the CNC biohybrids show almost no $^1O_2$ photoproduction in any solvent. This was thoroughly investigated and the underlying reason seems to be the severe loss of efficiency of oxygen trapping of the phthalocyanines' triplet state (^{3}Pc) upon anchoring to the CNC surface, a prerequisite for $^1O_2$ production. This is evidenced by the long ^{3}Pc lifetime in the biohybrids compared to the free molecules in solution (Figure 4; compare panels A vs E and B vs F) and by the minor effect of sodium azide, a potent $^1O_2$ quencher,[50] on the emission signals at 1275 nm (cf. panels C vs G and D vs H).

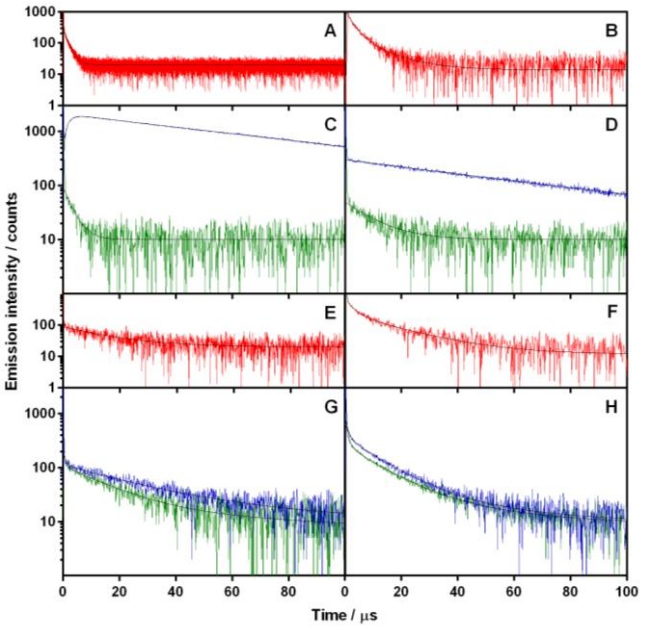

Figure 4. Comparison of the time-resolved near-IR emission signals in D_2O at 1110 nm (^{3}Pc; red line) and 1275 nm (^{3}Pc and $^1O_2$; blue line) for the free ZnPc **1** (A, C) and **2** (B, D), and for the biohybrids **1-CNC** (E, G) and **2-CNC** (F, H). The green line shows the effect of 50 mM NaN_3 on the 1275 nm emission. The ZnPc concentration was 3 mM in all cases.

It is worth mentioning that the signals at 1275 nm are a combination of ^{3}Pc phosphorescence and $^1O_2$ emission, as demonstrated by the remaining emission observed after adding sodium azide. The actual contribution of $^1O_2$ to the 1275 nm signals can thus be gauged by comparing the signals recorded in the absence and in the presence of azide. It is clear that it is much larger for the free molecules than for the CNC biohybrids, in which the 1275 nm signals are largely dominated by ^{3}Pc phosphorescence. The conclusion from these experiments is that anchoring the phthalocyanines to the CNC surface almost completely inhibits their ability to produce $^1O_2$. Similar results were observed in methanol and PBS (Figures S5 and S6, respectively). These results are consistent with the tight packing observed for the two ZnPc-CNC hybrids (see cryo-TEM results above), which limits the diffusion of molecular O_2 through the CNC bundles.[51] Thus only the ZnPc molecules in close contact with the solvent (i.e. located at the surface of those bundles) can effectively produce $^1O_2$. The different modes of packing observed for **1-CNC** and **2-CNC** do not alter this general picture.

In spite of the inhibited capacity of **1-CNC** and **2-CNC** for $^1O_2$ production in solution, the photodynamic inactivation properties of these new biohybrids were tested against *S. aureus* and *E. coli*, representative Gram-positive and Gram-negative bacteria, and *C. albicans*, a representative pathological yeast, showing excellent results that clearly outperformed those of the free ZnPc counterparts. Both **1-CNC** and **2-CNC** proved to be highly efficient in photoinactivating *S. aureus* (Figure 5A and B), resulting in 6 logs and 3 logs CFU reduction, respectively, at concentrations as low as 0.5 µM and light fluencies of only a few J/cm^2.

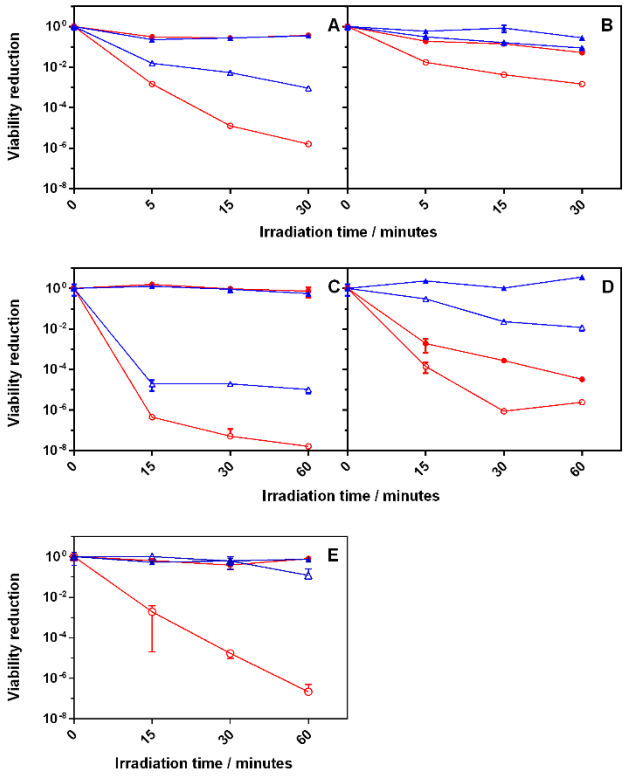

Figure 5. Photoinactivation of *S. aureus* (A and B) , *E. coli* (C and D) and *C. albicans* (E) upon red light irradiation (620-645 nm; 18 mW/cm^2). Working compounds concentrations: 0.5 µM in *S. aureus* and 3 µM in *E. coli* and *C. albicans* studies. **1-CNC** (left) and **2-CNC** (right) are represented with red lines and circle marks, while plain free **1** and **2** are depicted in blue with triangle marks. Dark controls are represented with solid marks.

Remarkably, both CNC hybrids showed a greater photoinduced antimicrobial effect than the free ZnPcs **1** and **2**, highlighting the importance of their formulation onto CNC. Furthermore, **1-CNC** is devoid of any dark toxicity, while that

of **2-CNC** is non-zero but almost negligible (1 log CFU reduction). Similar results were obtained against the Gram-negative *E. coli*, for which **1-CNC** showed no dark toxicity and reached an impressive 8 logs of CFU reduction, i.e., complete eradication, at approximately 3 mM and 64 J/cm^2 (Figure 5C). On the other hand, **2-CNC** induced up to 6 logs CFU reduction under the same conditions, yet its dark cytotoxicity was very high (4 log CFU reduction; Figure 5D). The free compounds were 3-4 logs less effective. Finally, **1** and **1-CNC** were also tested against *C. albicans* (Figure 5E), showing no dark toxicity. While compound **1** did not show any phototoxicity, **1-CNC** was highly phototoxic, reaching 6.5 logs CFU reduction at 3 mM and 64 J/cm^2. In sum, **1-CNC** is a very efficient and broad-spectrum photoantimicrobial agent, devoid of any dark toxicity and worth of further consideration.

An important final remark is that the PS concentrations and light doses applied for the photodynamic inactivation of both *S. aureus* and *E. coli* are one- to two order of magnitudes lower than those reported in the literature for similar, but covalently linked, porphyrin-based systems.[40,42] The substantial loss of $^1O_2$ photosensitisation ability of **1** and **2** when they are anchored to the CNC surface may explain the comparatively modest performance of the covalent systems. In the present case, on the contrary, the excellent photoantimicrobial ability of **1-CNC** and **2-CNC** suggest that the ZnPc molecules are transferred from the CNC surface to the microorganisms, stressing the importance of the followed supramolecular strategy. The low activity of the free ZnPc may be due to the strong aggregation of **1** and **2** in PBS, which may deter their binding to the cells. Likewise, the higher dark toxicity of **2-CNC**, particularly against *E. coli*, is probably related to a different localization in the cell wall.

Conclusions

In summary, we have studied supramolecular complexes of Pc molecules and CNC, as a type of optically active biohybrid nanostructures. Preparation of such materials represents a challenging goal from the nanotechnology point of view. Our strategy is based on the immobilization of cationic ZnPc derivatives onto unmodified CNC through an easy and straightforward non-covalent methodology, which is driven by electrostatic interactions. The resulting hybrids have been characterized by UV-Vis spectroscopy, DLS and cryo-TEM, proving that ZnPc stacking and CNC clustering are key processes that need to be prevented for an optimal photoinduced $^1O_2$ production. Importantly, $^1O_2$ is a key species in photodynamic therapy, water treatments, diagnostic arrays and photocatalytic technologies. The photodynamic inactivation of bacteria by **1-CNC** and **2-CNC**, for example, show clear advantages of these nanohybrids compared to the free ZnPc and to related nanosystems in which the photosensitiser is covalently linked to the CNC surface. The hybrids developed herein are therefore promising photoactive biomaterials, which may find useful applications in biomedicine and nanotechnology.

Experimental Section

Matrials and methods. All chemicals, except the ones specifically stated below, were purchased from Sigma-Aldrich and used without further purification. Uranyl acetate was purchased from Electron Microscopy Sciences. Anhydrous DMSO for singlet oxygen measurements was freshly distilled over $CaCl_2$. Sephadex® G-10 was purchased from GE Healthcare Bioscience. Cellite® filter cell was purchased from Sigma-Aldrich. TLC plates pre-coated with silica gel 60F254 were purchased from Merck. Column chromatography was carried out on Merck´s silica gel 60, 40-63 µm (230-400 mesh). ^{1}H-phenalen-1-one-2-sulphonic acid was synthesized as described previously.[52] ^{1}H and ^{13}C NMR spectra were recorded using Bruker AC-300 (^{1}H, 300 MHz; ^{13}C, 75 MHz) spectrometer, as solutions in deuterated solvents and using the solvent peak as internal standard. Mass spectra were performed on an ABSciex QSTAR apparatus equipped with an Agilent HPLC1100 injection system and electrospray ionizer. The UV-Vis absorbance spectra were measured using a Biotek Cytation 3 Imaging reader and a Take3 micro-volume plate or using a Varian Cary 6000i spectrophotometer, equipped with a 110 mm-diameter integrating sphere for transmittance measurements. Elemental analysis was carried out in a LECO CHNS-932 analyser. A Zetasizer Nano ZS90 analyzer (Malvern Instruments) with a He–Ne laser of 633 nm was used for measuring the particle size distributions, electrophoretic mobilities and ζ-potentials of pristine CNC, **1-CNC** and **2-CNC** at a 90° scattering angle. Disposable PMMA cuvettes (Plastibrand) were used for DLS measurements and Universal 'Dip' cell (ZEN1002) for ζ-potential measurements.

Synthesis of ZnPc 2. In a 10 mL sealed tube, ZnPc **4**[53] (30.1 mg, 12.6 µmol), whose structure is shown in Figure S1, was dissolved in 2-[2-(2-methoxyethoxy)ethoxy]ethyl iodide[54] (1.0 g, 3.65 mmol) and warmed up to 80 °C for 6 days under argon atmosphere. The reaction mixture was then poured in hexane. The obtained precipitate was filtered through cellite and collected with THF. After evaporation of the solvent under reduced pressure, the resultant solid was purified by size exclusion chromatography (Sephadex) using THF as eluent. The product was obtained as a green solid (49.5 mg, 84%). Characterization indicates an almost complete quaternization of the pyridine units (ca. 7 out of 8 groups within each molecule on average). Yet, the aqueous solubility of the compound is not diminished by such (ca. 10%) incomplete quaternization. ^{1}H-NMR (500 MHz, DMSO-d_6), d (ppm): 9.50 (s, 8H), 9.30 (s, 8H), 9.25 (s, 8H), 8.93 (s, 8H), 7.78 (d, J = 8.4 Hz, 16H), 7.50 (d, J = 8.4 Hz, 16H), 7.40

(d, J = 8.1 Hz, 2H), 7.01 (d, J = 8.1 Hz, 2H) 4.84 (s(br), 16H), 3.96 (s(br),16H), 3.56 (m, 16H), 3.42 (m, 16H), 3.30 (m, 16H), 3.17 (m, 16H), 3.02 (s, 24H), 1.25 (s, 56H). ^{13}C-NMR (126 MHz, DMSO-d_6), d (ppm): 156.9, 153.9, 153.3, 147.2, 141.3, 139.3, 138.0, 137.4, 134.6, 134.5, 133.8, 130.1, 130.0, 128.4, 128.0, 126.6, 125.9, 117.4, 71.5, 70.1, 70.0, 69.9, 69.0, 61.4, 58.4, 35.01 , 31.28. UV-Vis (DMSO): λ_{max}/nm (ε/dm^3 mol^{-1} cm^{-1}) = 335 (65500), 614 (26700), 657sh (42200) and 679 (169600). HRMS (ESI$^+$): *m/z* $[M+I]^{7+}$ calc. for $[C_{208}H_{256}N_{16}O_{32}ZnI]$ = 525.9609; found = 525.9700. $[M+2I]^{6+}$ calc. for $[C_{208}H_{256}N_{16}O_{32}ZnI_2]$ = 634.7712; found = 634.7778. $[M+3I]^{5+}$ calc. for $[C_{208}H_{256}N_{16}O_{32}ZnI_3]$ = 787.1064; found = 787.1095. $[M+4I]^{4+}$ calc. for $[C_{208}H_{256}N_{16}O_{32}ZnI_2]$ = 1015.3576; found = 1015.3579.

Synthesis of ZnPc-CNC hybrids. Pristine CNC dissolved in milli-Q water (3 mL, 5 mg mL^{-1}) were added to a solution of the corresponding ZnPc (12 mL, *ca.* 0.1 mM) and sonicated for 90 minutes. In the case of ZnPc **2**, for the previous dissolution in aqueous medium, it had to be first dissolved in a concentrated solution in DMSO (ca. 10 mM) and then rapidly injected into water, with a final DMSO proportion of less than 1%. After sonication of the mixture, the resulting dispersion was centrifuged at 10000 rpm (9391 rfc) for 10 minutes. The colored supernatant was removed and the pellet was washed by adding 10 mL of milli-Q water, re-dispersed by 2 minutes sonication and centrifuged for 10 extra minutes at 10000 rpm (9391 rfc). This procedure was repeated 5 times until no color was observed in the supernatant. After this procedure, the CNC were re-dispersed in the desired solvent.

Acknowledgements

AdlE acknowledges a Ramón y Cajal contract from the Spanish Ministry of Economy (MINECO). The work at Madrid was supported by the EU (SO2S, FP7-PEOPLE-2012-ITN, 316975; and CosmoPHOS-nano, FP7-NMP-2012-6, 310337-2), the Spanish MINECO (CTQ-2014-52869-P (TT) and CTQ-2014-53673-P (AdlE)) and Comunidad de Madrid (FOTOCARBON, S2013/MIT-2841). J.M., V.L. and M.A.K. acknowledge support through the Emil Aaltonen Foundation and the Academy of Finland (grants 267497, 273645 and 263504). This work was supported by the Academy of Finland through its Centres of Excellence Programme (2014-2019) and made use of the Aalto University Nanomicroscopy Centre (Aalto NMC). The work in Barcelona was supported by the Spanish MINECO (grant CTQ2013-48767-C3-1-R). R.B.-O. thanks the European Social Funds and the SUR del DEC de la Generalitat de Catalunya for his predoctoral fellowship (2016 FI_B1 00021)

Keywords: Phthalocyanine • Cellulose Nanocrystals • Photoantimicrobial Biohybrids

[1] J. A. A. W. Elemans, R. Van Hameren, R. J. M. Nolte, A. E. Rowan, *Adv. Mater.* **2006**, *18*, 1251–1266.

[2] H. Lu, N. Kobayashi, *Chem. Rev.* **2016**, DOI: 10.1021/acs.chemrev.5b00588.

[3] T. Basova, A. Hassan, M. Durmus, A. G. Gürek, V. Ahsen, *Coord. Chem. Rev.* **2016**, *310*, 131–153.

[4] M. V. Martínez-Díaz, G. de la Torre, T. Torres, *Chem. Commun. (Camb).* **2010**, *46*, 7090–108.

[5] N. Nishiyama, A. Iriyama, W.-D. Jang, K. Miyata, K. Itaka, Y. Inoue, H. Takahashi, Y. Yanagi, Y. Tamaki, H. Koyama, et al., *Nat. Mater.* **2005**, *4*, 934–941.

[6] N. Nishiyama, Y. Morimoto, W. D. Jang, K. Kataoka, *Adv. Drug Deliv. Rev.* **2009**, *61*, 327–338.

[7] A. Wang, L. Zhou, K. Fang, L. Zhou, Y. Lin, J. Zhou, S. Wei, *Eur. J. Med. Chem.* **2012**, *58*, 12–21.

[8] F. Setaro, R. Ruiz-González, S. Nonell, U. Hahn, T. Torres, *J. Inorg. Biochem.* **2014**, *136*, 170–176.

[9] F. Setaro, M. Brasch, U. Hahn, M. S. T. Koay, J. J. L. M. Cornelissen, A. de la Escosura, T. Torres, *Nano Lett.* **2015**, *15*, 1245–1251.

[10] D. Luque, A. D. La Escosura, J. Snijder, M. Brasch, R. J. Burnley, M. S. T. Koay, J. L. Carrascosa, G. J. L. Wuite, W. H. Roos, A. J. R. Heck, et al., *Chem. Sci.* **2014**, *5*, 575–581.

[11] M. Brasch, A. De La Escosura, Y. Ma, C. Uetrecht, A. J. R. Heck, T. Torres, J. J. L. M. Cornelissen, *J. Am. Chem. Soc.* **2011**, *133*, 6878–6881.

[12] M. R. Hamblin, G. Jori, *Photodynamic Inactivation of Microbial Pathogens: Medical and Environmental Applications*, RSC Publishing, London, **2011**.

[13] J. O'Neill, *Tackling Drug-Resistant Infections Globally: A Final Report and Recommendations*, **2016**.

[14] F. F. Sperandio, Y.-Y. Huang, M. R. Hamblin, *Recent Pat Antiinfect Drug Discov* **2013**, *8*, 1–23.

[15] M. R. Wainwright, M.; Maisch, T.; Nonell, S.; Plaetzer, K.; Almeida, A.; Tegos, G. P.; Hamblin, *Lancet Infect. Dis.* **n.d.**

[16] F. Dumoulin, M. Durmuş, V. Ahsen, T. Nyokong, *Coord. Chem. Rev.* **2010**, *254*, 2792–2847.

[17] M.-R. Ke, S.-L. Yeung, W.-P. Fong, D. K. P. Ng, P.-C. Lo, *Chem. - A Eur. J.* **2012**, *18*, 4225–4233.

[18] M. Mudyiwa, M. W. Ndinguri, S. a. Soper, R. P. Hammer, *J. Porphyr. Phthalocyanines* **2010**, *14*, 891–903.

[19] M. Mitsunaga, M. Ogawa, N. Kosaka, L. T. Rosenblum, P. L. Choyke, H. Kobayashi, *Nat. Med.* **2011**, *17*, 1685–1691.

[20] L. E. S. Contreras, J. Zirzlmeier, S. V. Kirner, F. Setaro, F. Martínez, S. Lozada, P. Escobar, U. Hahn, D. M. Guldi, T. Torres, *J. Porphyr. Phthalocyanines* **2015**, *19*, 320–328.

[21] R. Weijer, M. Broekgaarden, M. Kos, R. van Vught, E. A. J. Rauws, E. Breukink, T. M. van Gulik, G. Storm, M. Heger, *J. Photochem. Photobiol. C* **2015**, *23*, 103–131.

[22] M. Kryjewski, T. Goslinski, J. Mielcarek, *Coord. Chem. Rev.* **2015**, *300*, 101–120.

[23] P. Khoza, T. Nyokong, *J. Mol. Catal. A Chem.* **2015**, *399*, 25–32.

[24] P. Chauhan, N. Yan, *RSC Adv.* **2015**, *5*, 37517–37520.

[25] S. J. Eichhorn, A. Dufresne, M. Aranguren, N. E. Marcovich, J. R. Capadona, S. J. Rowan, C. Weder, W. Thielemans, M. Roman, S.

Renneckar, et al., *J. Mater. Sci.* **2010**, *45*, 1–33.
[26] Y. Habibi, L. a. Lucia, O. J. Rojas, *Chem. Rev.* **2010**, *110*, 3479–3500.
[27] J. R. McKee, E. A. Appel, J. Seitsonen, E. Kontturi, O. A. Scherman, O. Ikkala, *Adv. Funct. Mater.* **2014**, *24*, 2706–2713.
[28] R. J. Moon, A. Martini, J. Nairn, J. Simonsen, J. Youngblood, *Chem. Soc. Rev.* **2011**, *40*, 3941–3994.
[29] M. Pääkkö, J. Vapaavuori, R. Silvennoinen, H. Kosonen, M. Ankerfors, T. Lindström, L. A. Berglund, O. Ikkala, *Soft Matter* **2008**, *4*, 2492–2499.
[30] H. Rosilo, E. Kontturi, J. Seitsonen, E. Kolehmainen, O. Ikkala, *Biomacromolecules* **2013**, *14*, 1547–1554.
[31] Y. Habibi, *Chem. Soc. Rev.* **2014**, *43*, 1519–1542.
[32] N. Lin, A. Dufresne, *Biomacromolecules* **2013**, *14*, 871–880.
[33] M. L. Hassan, C. M. Moorefield, H. S. Elbatal, G. R. Newkome, *J. Macromol. Sci. Part A* **2012**, *49*, 298–305.
[34] M. L. Hassan, C. M. Moorefield, H. S. Elbatal, G. R. Newkome, D. a. Modarelli, N. C. Romano, *Mater. Sci. Eng. B* **2012**, *177*, 350–358.
[35] H. Rosilo, J. McKee, E. Kontturi, T. Koho, V. Hytönen, O. Ikkala, M. A. Kostiainen, *Nanoscale* **2014**, 11871–11881.
[36] N. Drogat, R. Granet, C. Le Morvan, G. Bégaud-Grimaud, P. Krausz, V. Sol, *Bioorg. Med. Chem. Lett.* **2012**, *22*, 3648–3652.
[37] W. Wu, F. Huang, S. Pan, W. Mu, X. Meng, H. Yang, *J. Mater. Chem. A* **2015**, *3*, 1995–2005.
[38] L. Jin, W. Li, Q. Xu, Q. Sun, *Cellulose* **2015**, *22*, 2443–2456.
[39] J. W. Grate, K.-F. Mo, Y. Shin, A. Vasdekis, M. G. Warner, R. T. Kelly, G. Orr, D. Hu, K. J. Dehoff, F. J. Brockman, et al., *Bioconjug. Chem.* **2015**, *26*, 593–601.
[40] E. Feese, H. Sadeghifar, H. S. Gracz, D. S. Argyropoulos, R. A. Ghiladi, *Biomacromolecules* **2011**, *12*, 3528–3539.
[41] N. Drogat, R. Granet, V. Sol, C. Le Morvan, G. Begaud-Grimaud, F. Lallouet, P. Krausz, *Photodiagnosis Photodyn. Ther.* **2011**, *8*, 157.
[42] B. L. Carpenter, E. Feese, H. Sadeghifar, D. S. Argyropoulos, R. A. Ghiladi, *Photochem. Photobiol.* **2012**, *88*, 527–536.
[43] C. D. Edgar, D. G. Gray, *Cellulose* **2003**, *10*, 299–306.
[44] H. Li, T. J. Jensen, F. R. Fronczek, M. G. Vicente, *J.Med.Chem.* **2008**, *51*, 502–511.
[45] J. W. Ryan, E. Anaya-Plaza, A. D. La Escosura, T. Torres, E. Palomares, *Chem. Commun.* **2012**, *48*, 6094–6096.
[46] T. Nyokong, *Coord. Chem. Rev.* **2007**, *251*, 1707–1722.
[47] J. O. Zoppe, L.-S. Johansson, J. Seppälä, *Carbohydr. Polym.* **2015**, *126*, 23–31.
[48] S. Jiménez-Banzo, A.; Ragàs, X.; Kapusta, P.; Nonell, *Photochem. Photobiol. Sci.* **2008**, *7*, 1003–1010.
[49] P. R. Ogilby, C. S. Foote, *J. Am. Chem. Soc.* **1983**, *105*, 3423–3430.
[50] M. Y. Li, C. S. Cline, E. B. Koker, H. H. Carmichael, C. F. Chignell, P. Bilski, *Photochem. Photobiol.* **2001**, *74*, 760–764.
[51] A. J. Svagan, C. Bender Koch, M. S. Hedenqvist, F. Nilsson, G. Glasser, S. Baluschev, M. L. Andersen, *Carbohydr. Polym.* **2016**, *136*, 292–299.
[52] S. Nonell, M. González, F. R. Trull:, *Afinidad,* **1993**, *44*, 445–450.
[53] E. Anaya-Plaza, M. M. Oliva, A. Kunzmann, C. Romero-Nieto, R. D. Costa, A. De La Escosura, D. M. Guldi, T. Torres, *Adv. Funct. Mater.* **2015**, *25*, 7418–7427.
[54] B. B.-A. Bar-Nir, J. F. Kadla, *Carbohydr. Polym.* **2009**, *76*, 60–67.

Entry for the Table of Contents

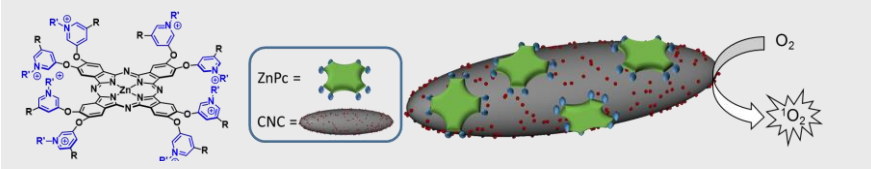

Photoantimicrobial biohybrids are easily produced by the non-covalent immobilization of cationic phthalocyanines onto the surface of sulphated cellulose nanocrystals through electrostatic interactions, resulting in a well-defined and highly efficient nanostructured photosensitizing system.

Eduardo Anaya-Plaza, Eveline van de Winckel, Joona Mikkilä, Jani-Markus Malho, Olli Ikkala, Oscar Gulías, Roger Bresolí-Obach, Montserrat Agut, Santi Nonell, Tomás Torres, Mauri A. Kostiainen* and Andrés de la Escosura**

Page No. – Page No.

Photoantimicrobial Biohybrids by Supramolecular Immobilization of Cationic Phthalocyanines onto Cellulose Nanocrystals